16 July 1999

Drift Velocity of Free Electrons in Liquid Argon

W. Walkowiak

Institut für Physik, Universität Mainz, D-55099 Mainz, Germany

ATL-LARG-99-008
30/07/99

Abstract

A measurement of the drift velocity of free electrons in liquid argon has been performed. Free electrons have been produced by photoelectric effect using laser light in a so called "laser chamber". The results on the drift velocity v_d are given as a function of the electric field strength in the range 0.5 kV/cm $\leq |\vec{E}| \leq$ 12.6 kV/cm and the temperature in the range 87 K $\leq T \leq$ 94 K. A global parametrization of $v_d(|\vec{E}|, T)$ has been fitted to the data. A temperature dependence of the electron drift velocity is observed, with a mean value of $\Delta v_d/(\Delta T\, v_d) = (-1.72 \pm 0.08)\%/\mathrm{K}$ in the range of $87 - 94$ K.

Key words: liquid argon, electron drift velocity, calorimetry

1 Introduction

The ATLAS-experiment [1] at CERN's future Large Hadron Collider (LHC) makes use of liquid argon sampling calorimeters. The initial current readout method [2] is adopted in order to cope with the short bunch crossing time of 25 ns. Since the current signal I_0 is proportional to the velocity v_d of the drifting electrons I_0, the calorimeter response is sensitive to changes in the drift velocity.

The drift velocity depends primarily on the electric field strength. A weaker dependence on the temperature of the liquid argon is expected. In addition, it is affected by molecules in the liquid like carbon hydroxides, which lead to an increase of v_d [3–6]. Electronegative impurities like oxygen on the other hand reduce the number of drifting electrons due to attachment processes, but do not change the drift velocity.

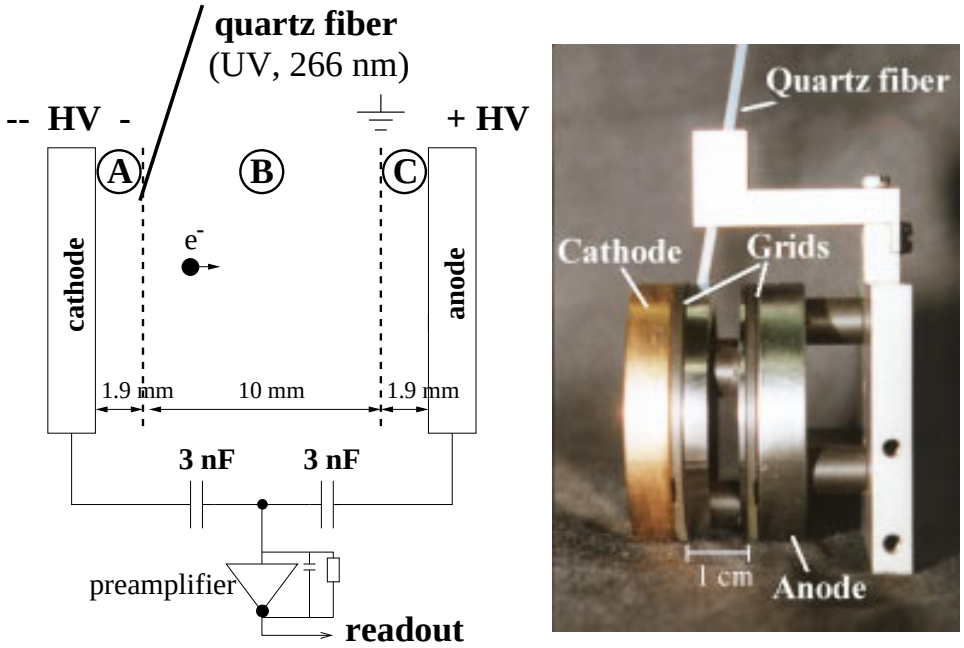

Fig. 1. *Schematic view (left) and photograph (right) of the laser chamber. The three drift sections A, B and C are indicated.*

Earlier measurements of the electron drift velocity in liquid argon [7,3] in which a wide range of electric fields (0.01 kV/cm $\leq |\vec{E}| \leq$ 100 kV/cm) were covered are inconsistant and cannot be brought into agreement if temperature effects are corrected for. Given the importance of the exact knowledge of the dependence of the drift velocity on the electric field and temperature to achieve a smal constant term in the calorimeter energy resolution, a new measurement has been performed.

The monitor used to perform this measurement ("laser chamber") was developed in the context of the purity monitoring effort for the ATLAS liquid argon calorimeters [8]. From a signal analysis, the electron life time τ and the drift velocity can be obtained simultanously. The electron life time τ represents an absolute measure for the concentration of electronegative impurities where the transformation can be done according to [9].

First, a short description of the experimental set-up and the working principle of the "laser chamber" is given. Second, the measurement of the drift velocity and the discussion of systematical uncertaincies is presented, followed by the final result on the dependence of the drift velocity on the electric field strength and temperature. Finally, a comparision with measurements done previously by different groups is shown.

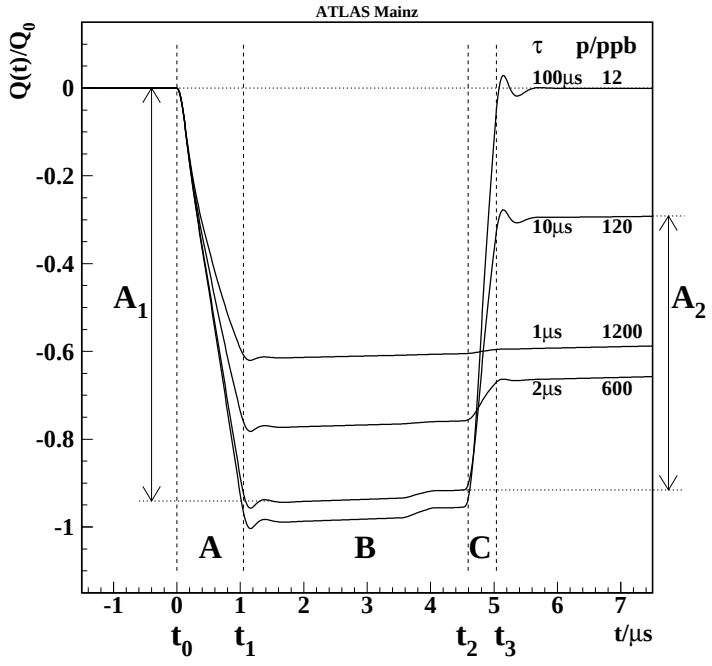

Fig. 2. *Simulated laser chamber waveforms for different values of the electron life time τ at an electric field strength of $|\vec{E}_B| = 2.5$ kV/cm. The corresponding impurity concentrations in ppm oxygen equivalents are calculated according to [9].*

2 Experimental setup

2.1 Laser chamber

Figure 1 shows a schematic view and a photograph of the laser chamber designed similarly to one used in [10]. Pulses of UV-laser light guided to the gold-coated cathode by a quartz fiber produce electrons via the photoelectric effect at the cathode. As the electrons drift towards the andode due to the electric field they pass two grids: the cathode and the anode grid, which devide the cell into three sections of 1.9, 10 and 1.9 mm length, respectively. The grids electrostatically shield the middle drift section from the cathode and the anode, which are connected to the same charge sensitive preamplifier by decoupling capacitors. The four electrodes define an increasing electric field; the field ratios $|\vec{E}_A|/|\vec{E}_B|$ and $|\vec{E}_B|/|\vec{E}_C|$ at the grids have to be adjusted (to typically 1:3) to allow for optimal transparency [11,12]. The output voltage of the preamplifier, induced by the drifting electrons, is recorded by means of a digital oscilloscope. Figure 2 shows the expected waveforms for different impurity concentrations, which result from a convolution of the ideal laser chamber signal function with the response function of the preamplifier. The latter was measured and parameterized separately [12]. The drift velocity is measured

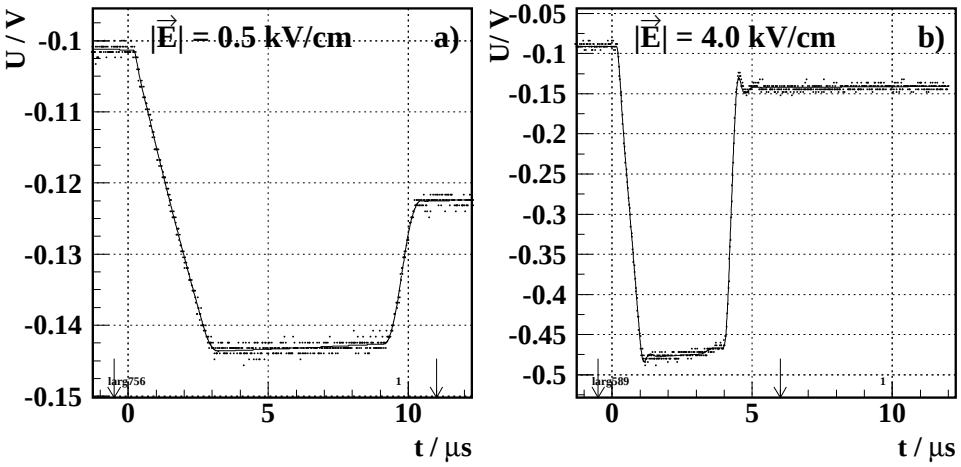

Fig. 3. *Signals of the laser chamber for two extreme values of the electric field strength* $|\vec{E}_B|$ *of a)* 0.5 kV/cm *and b)* 4 kV/cm. *At higher field strength a smaller drift time is observed. The results of the fit to the model function are superimposed.*

from the drift times between the grids and in the third drift section (anode side). To first order, neglecting electron attachment in the outer sections, the electron life-time is a function of the amplitude ratio A_2/A_1 (see Fig. 2). The complete model function is fitted to the data with the drift times and the electron life-time being free parameters. Examples are shown in Figure 3. Details of the pulse shape depend also on the finite width of the electron cloud and the reflection of some laser light onto the cathode grid. These effects are taken into account in the model function. For example, the latter effect gives rise to a small step in the signal section B (Fig. 2), which has been observed in the data (Fig. 2).

2.2 Local cryogenic environment

Liquid argon is produced inside a cryostat by condensing gaseous argon utilizing a liquid nitrogen cooling loop. Prior to cool down the system is evacuated (typically to 10^{-7} mbar) and rinsed with argon gas several times. Oxygen- and water admixtures in the gaseous argon are reduced by special adsorbers [1] before entering the cryostat. The liquified argon is collected in in a 4 liter volume into which the laser chamber is suspended.

After completion of the condensing, a pressure controled cooling loop is used to compensate for the heat entering the cryostat. As the pressure of the argon

[1] Hydrosorb and Oxisorb devices produced by Messer-Griesheim.

gas varies with the cooling cycles there is a slight temperature variation in the liquid of typically ± 0.03 K. Together with the uncertaincy of the calibrated Pt100-temperature probe [2] suspended into the liquid argon, the total systematical error on the temperature measurement is evaluated to ± 0.05 K [12].

3 Analysis of the data

3.1 Determination of the drift velocity

The electric field strength $|\vec{E}_B|$ in the middle drift section and the temperature T were varied in steps of 0.25 kV/cm in the range of 0.5 kV/cm $\leq |\vec{E}_B| \leq$ 4.0 kV/cm and in steps of 1 K in the range of 87 K $\leq T \leq$ 94 K, respectively. At each point about 20 waveforms were recorded and fitted individually. The accessible electric field range can be enlarged by measuring the drift time in the third drift section in addition. In this section a field range between 1.6 kV/cm and 12.6 kV/cm can be covered. This allows for both overlap and a large extension compared to the measurement in the middle section. The mean drift times t_B and t_C, obtained by averaging the individual fit results at each point in ($|\vec{E}|$,T) are used to calculate the drift velocities v_B and v_C for the second and third section, respectively, according to $v_{B,C} = d_{B,C}/t_{B,C}$.

Figure 4 shows the measured drift velocities for the two extreme temperature values.

In order to parameterize the drift velocity as a function of $|\vec{E}|$ and T, the following empirical function (c.f. [13]) is fitted to the data points:

$$v_d(T, |\vec{E}|) = (P_1 (T - T_0) + 1) \left(P_3 |\vec{E}| \ln \left(1 + \frac{P_4}{|\vec{E}|} \right) + P_5 |\vec{E}|^{P_6} \right) + P_2 (T - T_0) \ . \quad (1)$$

The parameters $P_1, \ldots, P_6$ are obtained from a global χ^2-fit to all data from both drift sections. The reference temperature T_0 is chosen to be 90.371 K, the mean value of the temperature of all data points used. The resulting set of parameters is summarized in Table 1 and the fit results are superimposed on Figure 4 for the temperatures indicated.

[2] PT103, LakeShore Cryotronics Inc.; readout device: DP95 Digital RTD Thermometer, Omega Engineering Inc.

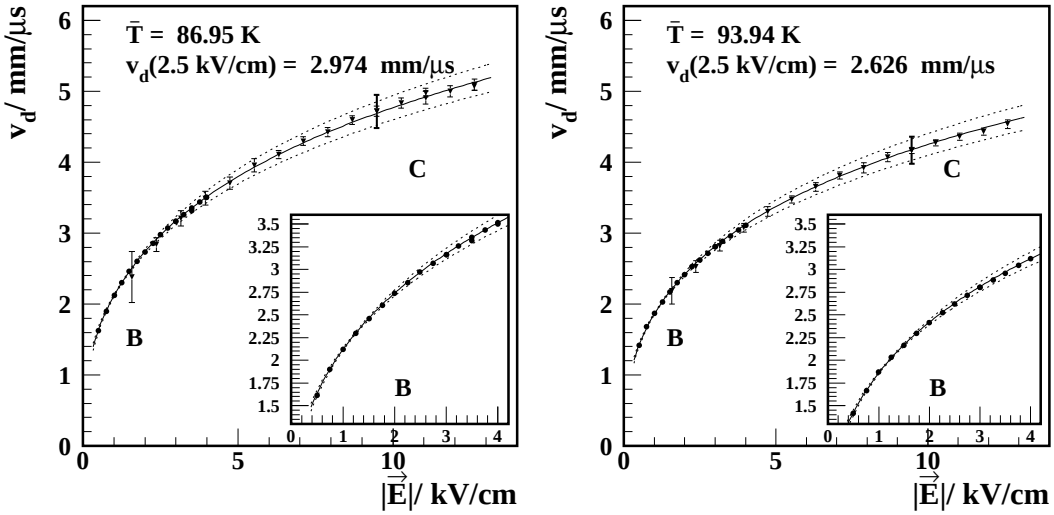

Fig. 4. *The drift velocity v_d as a function of $|\vec{E}|$ for the second (B) and third (C) section at 87 K and 94 K. Statistical errors are indicated; as an example the total error of an individual data point is shown at $|\vec{E}| = 9.5$ kV/cm. The result of the global fit of (1) to the data points is superimposed together with an error band which includes the correlations among the data points. The mean temperature for the data points in each figure is given.*

parameter	**value**			
P_1	-0.01481	$\pm$	0.00095	K^{-1}
P_2	-0.0075	$\pm$	0.0028	K^{-1}
P_3	0.141	$\pm$	0.023	$\left(\frac{\mathrm{kV}}{\mathrm{cm}}\right)^{-1}$
P_4	12.4	$\pm$	2.7	$\left(\frac{\mathrm{kV}}{\mathrm{cm}}\right)$
P_5	1.627	$\pm$	0.078	$\left(\frac{\mathrm{kV}}{\mathrm{cm}}\right)^{-P_6}$
P_6	0.317	$\pm$	0.021	
T_0	90.371		(fixed)	K

Table 1
Result of the global fit of parametrization (1) to the total set of data points from the second and third drift section. The correlations in the data have been properly taken into account.

3.2 Systematical uncertaincies

The error at each point is dominated by systematic uncertaincies. The following effects contribute: uncertaincies in the determination of the drift times,

the accuracy of the measurement of the drift distances, uncertaincies in the temperature measurement and in the knowledge of the electric field strength.

Systematical uncertaincies in the parameter fit of the drift times have been investigated using both fits to the data with constrained parameters and fits to simulated data in which the parameter describing the effect of interest has been varied [12]. External noise, observed in the regime of about 100 Hz to 1000 Hz, is found to contribute less than $\pm 0.1\%$ ($\pm 1.0\%$) relative error on the drift time in the middle (third) drift section for $|\vec{E}| \geq 2.5$ kV/cm (7.9 kV/cm) and about $\pm 1.0\%$ ($\pm 10\%$) for $|\vec{E}| = 0.5$ kV/cm (1.6 kV/cm). The variation of the extension of the charge cloud in drift direction by about $\pm 10\%$ yields the other major contribution to the relative error on the drift time of less than $\pm 0.3\%$ ($\pm 3.0\%$) in the domain of higher field strength and about $\pm 0.4\%$ ($\pm 5.0\%$) at the lowest field strength. The contributions to the error on the drift time measurement due to the choice of parameters in the model function describing the preamplifier's response and due to the granularity of the digitilization are small compared to the two major effects discussed above. Even the decrease of the electron life-time from about 23 μs to about 10 μs only gives rise to a negligible effect according to studies with simulated waveforms. Adding all effects in quadrature, the relative error on the measured drift times in the middle (third) drift section amounts to about $\pm 0.4\%$ ($\pm 3.6\%$) for $|\vec{E}| \geq$ 2.5 kV/cm (7.9 kV/cm) and to about $\pm 1.4\%$ ($\pm 20\%$) for $|\vec{E}| = 0.5$ kV/cm (1.6 kV/cm).

The inaccuracy in the determination of the drift distances of ± 0.1 mm causes a contribution $\pm 0.65\%$ ($\pm 3.6\%$) to the relative error on the measured drift velocity in the middle (third) drift section. Together with the systematical error arising from the determination of the drift time, this contribution dominates the total systematical error.

The uncertaincy of the temperature determination for one data set amounts to $\Delta T \approx \pm 0.05$ K (c.f. section 2.2). This corresponds to a contribution of less than ± 0.07 % to the relative error on the drift velocity, which is negligible.

Also, the uncertaincy in the knowledge of the electric field strength is estimated to contribute less than ± 0.2 % (± 0.7 % at very low field strength) to the relative error on the drift velocity.

In total, for the second (third) drift section the relative error on v_d due to systematic uncertaincies amounts to about $\pm 0.8\%$ ($\pm 5\%$) for $|\vec{E}| \geq 2.5$ kV/cm (7.9 kV/cm). At very low values of the electric field strength the relative error rises to $\pm 2.1\%$ ($\pm 32\%$). Thus, the systematic uncertaincies by far dominate the statistical error of typically $\pm 0.2\%$ ($\pm 2.0\%$) in the middle (third) drift section.

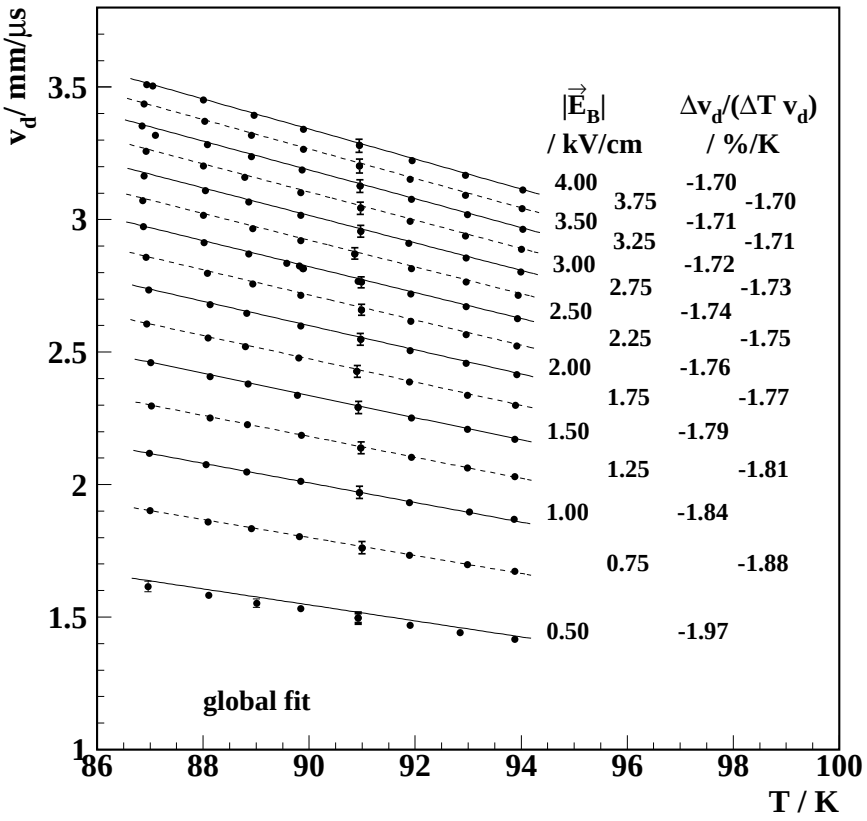

Fig. 5. *The electron drift velocity v_d (in the second drift section) as a function of the temperature T for different values of the electric field strength $|\vec{E}_B|$. The result of the global fit of (1) to the data points is superimposed. Except for the data points at $T = 91$ K, where the total error on the individual v_d value is shown, only statistical error bars are included.*

For the global χ^2-fit of parametrization (1) correlations among the (systematical) errors were properly taken into account. The resulting one sigma error band is shown in Figure 4.

3.3 Final results

As can be seen in Figure 4, the parametrization adopted describes well the drift velocity measured as function of $|\vec{E}|$. The drift velocity rises with $|\vec{E}|$ as expected. Comparing both plots a decrease of v_d with increasing temperature is observed.

As shown in Figure 5, the drift velocity v_d is a linear function of the temperature as taken into account by P_1 and P_2 in parametrization (1). The relative change in the drift velocity $\Delta v_d/(\Delta T\, v_d)$ obtained slightly increases from -1.64%/K at $|\vec{E}| = 12.6$ kV/cm to -1.97%/K at $|\vec{E}| = 0.5$ kV/cm considering both the data of the second and third drift section together. The mean

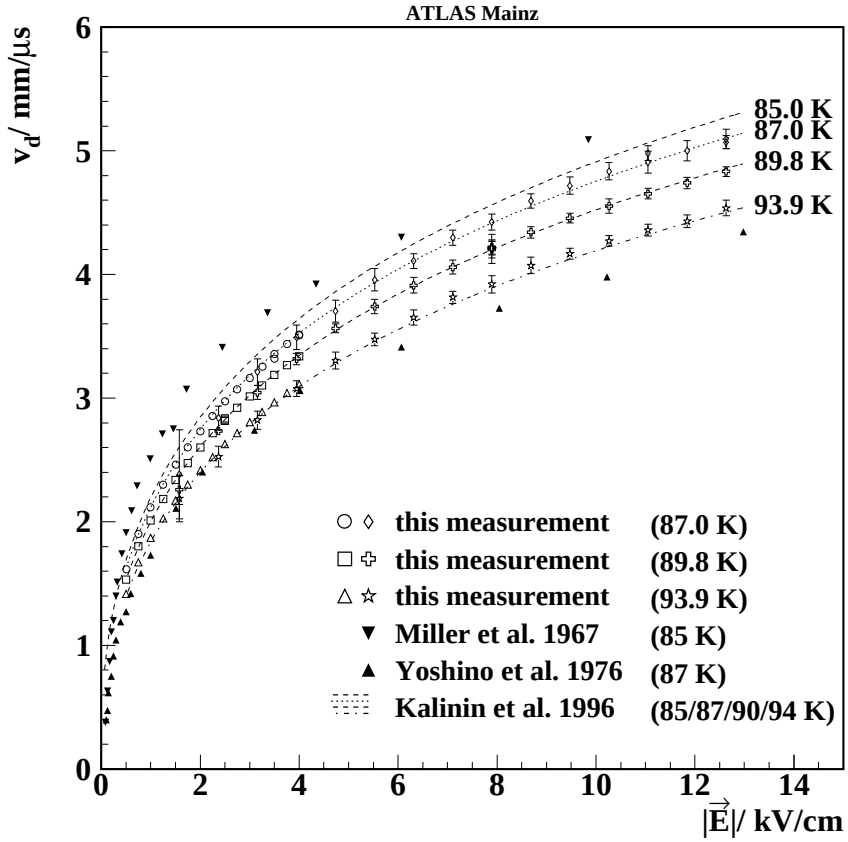

Fig. 6. *Drift velocity v_d as a function of $|\vec{E}|$ for the second (○ □ △) and third (◊ ✣ ☆) drift section. This measurement (open symbols, statistical errors only), shown for three different temperatures, is compared to the parametrization of Kalinin et al. [13]. A clear deviation of the older measurements of Miller et al. [7] (▼) and Yoshino et al. [3] (▲) is observed.*

value of the temperature dependence in the $|\vec{E}|$-range considered is measured to be

$$\frac{\Delta v_d}{\Delta T\, v_d} = (-1.72 \pm 0.08)\%/\mathrm{K}\,.$$

4 Comparison with previous measurements

In Figure 6 this measurement is compared to three earlier measurements, which were based on different methods. Whereas the presented measurement agrees with the one of Ref. [13], there is a clear disagreement with Ref. [7,3]:

- **Miller et al.** [7] used a pulsed 40 keV electron gun to ionize the liquid argon in a gap of 0.1 to 0.6 mm width. The electron life time and temperature quoted were approximately 10 μs and (85.0 ± 0.3) K. The drift velocities measured are about 13% larger than expected from the parametrization obtained here, if evaluated at 85 K.
- **Yoshino et al.** [3] produced free electrons in a 1 mm gap by pulsed bombardment of the drift-cell with 15 MeV bremsstrahlung from an electron accelerator. They quote an electron life time larger than 5 μs and a temperature of 87 K. The electron drift velocities obtained are about 18% smaller compared to the presented measurement's prediction at 87 K.
- **Kalinin et al.** [13] at CERN used a laser chamber with a simple geometry without grids and a gap of 10 mm. The quartz fiber focussing the UV-laser light on the cathode was mounted in a central hole of the anode. A fit to the signal of a current sensitive preamplifier was used to extract the drift time across the gap and the electron life-time. The electron life-time was measured to about 120 μs. The drift velocity data taken in the ranges $T = 86.8 - 97.6$ K and $|\vec{E}| = 0.5 - 7.5$ kV/cm are given as a fit to parametrization (1). As shown in Fig. 6, good agreement with the current measurement is obtained.

To summarize, good agreement between the present measurement and the one of reference [13] is found. It should be stressed that in both cases the electrons are produced via photo effect and therefore no positive ions, which may disturb the measurement, exist in the drift sections. In contrast, the measurements [7,3], where the drift charges are obtained by ionization of the liquid argon, show clear discrepancies.

5 Conclusions

The measurement of the drift velocity of free electrons in liquid argon as a function of electric field strength and temperature $v_d(|\vec{E}|, T)$ has been performed. The data are well described by parametrization (1). An average temperature gradient of v_d has been measured to be:

$$\frac{\Delta v_d}{\Delta T \, v_d} = (-1.72 \pm 0.08)\%/\mathrm{K} \, .$$

Since this is a relatively large effect, a precise, local measurement of the liquid argon temperature in the liquid argon calorimeters of the ATLAS experiment is required in order to keep the influence of the uncertaincy in v_d on the constant term of the calorimeter resolution as small as possible.

Acknowledgements

Financial support from the German Bundesministerium für Bildung, Wissenschaft, Forschung und Technologie, under contract number FKZ 05 7MZ18 P4, is acknowledged. I also wish to thank the members of the purity group at Mainz and J. Bremer, A. Gonidec and G. Kesseler at CERN for their support and helpful discussions.

References

[1] ATLAS Collaboration: Technical Proposal, CERN/LHCC/94-43 LHCC/P2 (1994).

[2] C. Cerri et al., NIM 227 (1984) 227–236,
V. Radeka et al., NIM A 265 (1988) 228.

[3] K. Yoshino et al., Phys. Rev. A 14 (1976) 438–444.

[4] D.W. Swan, Proc. Phys. Soc. 82 (1963) 74.

[5] D.W. Swan, Proc. Phys. Soc. 83 (1964) 659–666.

[6] E. Shibamura et al., NIM 131 (1975) 2490.

[7] L.S. Miller et al., Phys. Rev. 166, 3 (1968) 871.

[8] ATLAS Collaboration: Liquid Argon Calorimeter Technical Design Report, CERN/LHCC/96-41 (1996).

[9] W. Hofmann et al., NIM A135 (1976) 151.

[10] G. Carugno et al., NIM A292 (1990) 580–584.

[11] O. Bunnemann et al., Can. J. Research A 27 (1949).

[12] W. Walkowiak, *Entwicklung von Flüssig-Argon-Reinheitsmeßgeräten für das ATLAS-Experiment und Messungen zur Energieauflösung eines hadronischen Flüssig-Argon-Kalorimeters*, Dissertation Mainz (1998), (in German);
and references therein.
Online available at:
http://atlasinfo.cern.ch/Atlas/documentation/thesis/thesis.html

[13] A.M. Kalinin et al., ATLAS Internal Note, ATLAS-LARG-NO-058, CERN (1996).